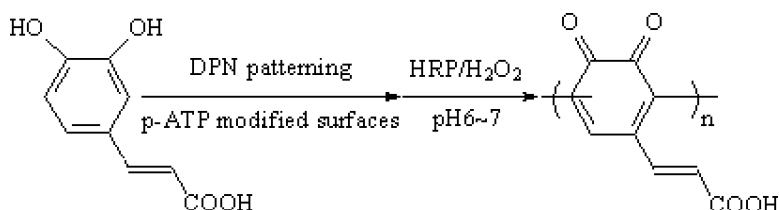


Peroxidase-Catalyzed in Situ Polymerization of Surface Orientated Caffeic Acid

Peng Xu, Hiroshi Uyama, James E. Whitten, Shiro Kobayashi, and David L. Kaplan

J. Am. Chem. Soc., **2005**, 127 (33), 11745-11753 • DOI: 10.1021/ja051637r • Publication Date (Web): 28 July 2005

Downloaded from <http://pubs.acs.org> on March 25, 2009



More About This Article

Additional resources and features associated with this article are available within the HTML version:

- Supporting Information
- Links to the 6 articles that cite this article, as of the time of this article download
- Access to high resolution figures
- Links to articles and content related to this article
- Copyright permission to reproduce figures and/or text from this article

[View the Full Text HTML](#)

Peroxidase-Catalyzed in Situ Polymerization of Surface Orientated Caffeic Acid

Peng Xu,[†] Hiroshi Uyama,[‡] James E. Whitten,[§] Shiro Kobayashi,[‡] and David L. Kaplan^{*†}

Contribution from the Departments of Biomedical Engineering and Chemical & Biological Engineering, Bioengineering & Biotechnology Center, Tufts University, Medford, Massachusetts 02155, Department of Materials Chemistry, Graduate School of Engineering, Kyoto University, Kyoto 615-8510, Japan, and Department of Chemistry and Center for Advanced Materials, University of Massachusetts—Lowell, Lowell, Massachusetts 01854

Received March 15, 2005; E-mail: david.kaplan@tufts.edu

Abstract: Nanoscale surface patterning and polymerization of caffeic acid on 4-aminothiophenol-functionalized gold surfaces has been demonstrated with dip pen nanolithography (DPN). The diphenolic moiety of caffeic acid can be polymerized by biocatalysis with laccase or horseradish peroxidase. In the present study, the DPN patterned features were polymerized in situ through the use of the peroxidase. Using samples prepared by DPN, microcontact printing, and adsorption on macroscopic substrates, the products were characterized by electrostatic force microscopy (EFM), MALDI-TOF, X-ray photoelectron spectroscopy (XPS), UV–vis, and FT-IR. The in situ surface polymerization resulted in the formation of a quinone structure, while the phenyl ester formed in bulk polymerization reactions was not detected. A different coupling site was observed when comparing the polymers obtained from solution (bulk) vs the surface DPN reactions. The structural differences were attributed to surface-induced preorganization and orientation of the monomers prior to the enzymatic polymerization step. The results of this study expand the application of DPN technology to surface modification and surface chemistry reactions wherein stereoregularity and regioselectivity can be exploited.

Introduction

Enzyme-based reactions are often carried out under ambient conditions, such as neutral pH, room temperature, and in aqueous or nontoxic solvents. In the past few years, a number of studies of enzymatic polymerization have focused on phenolic monomers for polymer resins.^{1–4} Recently, catechol derivatives have attracted attention because of their diphenolic structure that can be oxidized and then polymerized by the action of horseradish peroxidase (HRP) and laccase.⁵ The polymer resins obtained in these reactions can be further functionalized by controllable oxidation, cross-linking, or grafting.⁶ Another application for these types of enzymatic reactions is the conversion of renewable resources into value-added products, such as by treatment with tyrosinase.^{7,8} A large number of catechol derivatives are nontoxic, water-soluble, natural products with potential green chemistry benefits, an advantage when

compared to traditional phenolic materials used in resin forming reactions.

Dip pen nanolithography (DPN) is a convenient method to perform surface patterning on the nanometer length scale.^{9,10} Initially, the ink and corresponding substrates used in DPN were limited to small organic thiols, such as 16-mercaptohexadecanoic acid (MHA) and 1-octadecanethiol (ODT), on gold surfaces. The use of DPN has rapidly expanded in recent years. Electrochemical dip pen nanolithography (E-DPN) was developed by applying electrochemical methods to create reactive lithography. By using the DPN technique, varieties of biomacromolecules, such as peptides, proteins and DNA, have been patterned on modified gold or silicon surfaces to study nanostructures, biophysical properties, or molecular recognition.^{11–14} Further, reactive materials and initiators have been patterned to induce surface reactions and polymerization.^{15,16} The use of DPN is not restricted to making patterns or arrays; the SPM tip

[†] Tufts University.

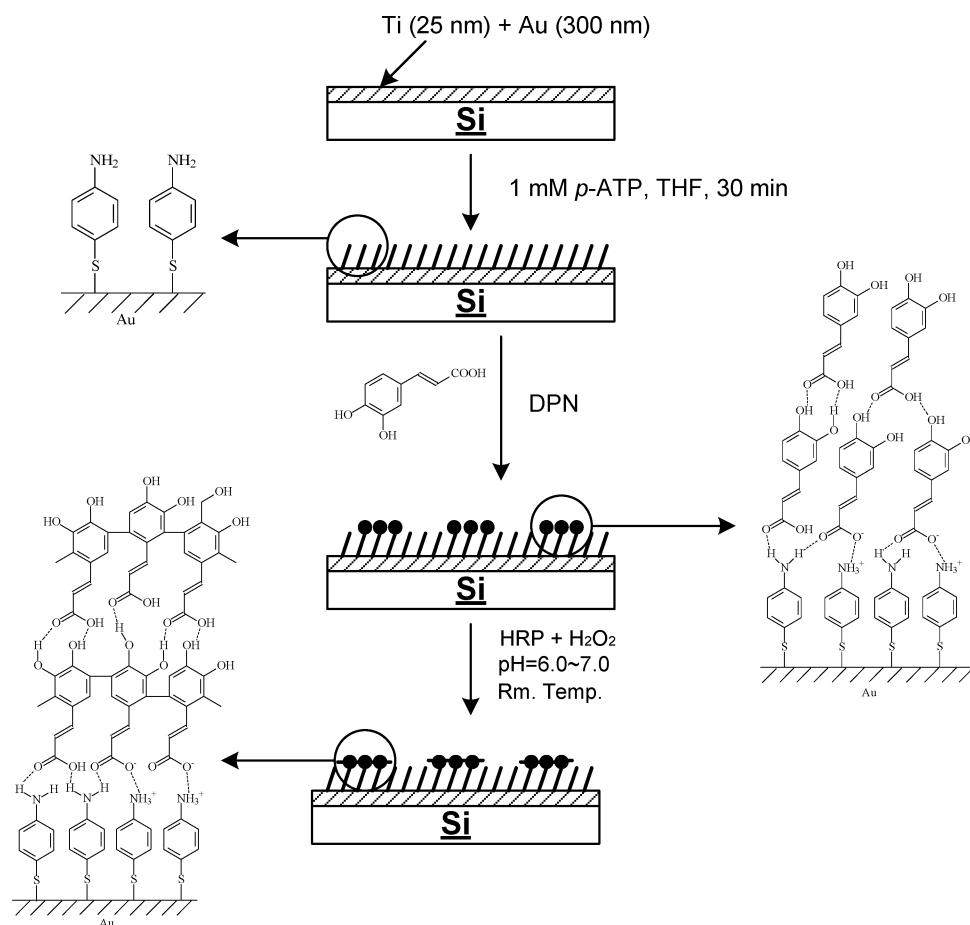
[‡] Kyoto University.

[§] University of Massachusetts—Lowell.

- (1) Reihmann, M. H.; Ritter, H. *J. Macromol. Sci. Pure Appl. Chem.* **2002**, *A39*, 1369.
- (2) Kobayashi, S.; Uyama, H.; Kimura, S. *Chem. Rev.* **2001**, *101*, 3793.
- (3) Fukuoka, T.; Uyama, H.; Kobayashi, S. *Macromolecules* **2003**, *36*, 8213.
- (4) Reihmann, M. H.; Ritter, H. *Macromol. Biosci.* **2001**, *1*, 85.
- (5) Aktas, N.; Sahiner, N.; Kantoglu, O.; Salih, B.; Tanyolac, A. *J. Polym. Environ.* **2003**, *11*, 123.
- (6) Fukuoka, T.; Uyama, H.; Kobayashi, S. *Macromolecules* **2004**, *37*, 5911.
- (7) Aberg, C. M.; Chen, T.; Payne, G. F. *J. Polym. Environ.* **2002**, *10*, 77.
- (8) Wu, L.-Q.; Embree, H. D.; Balgley, B. M.; Smith, P. J.; Payne, G. F. *Environ. Sci. Technol.* **2002**, *36*, 3446.

- (9) Piner, R. D.; Zhu, J.; Xu, F.; Hong, S.; Mirkin, C. A. *Science* **1999**, *283*, 661.
- (10) Hong, S.; Zhu, J.; Mirkin, C. A. *Science* **1999**, *286*, 523.
- (11) Wilson, D. L.; Martin, R.; Hong, S.; Cronin-Golomb, M.; Mirkin, C. A.; Kaplan, D. L. *Proc. Natl. Acad. Sci. U. S. A.* **2001**, *98*, 13660.
- (12) Lim, J.-H.; Ginger, D. S.; Lee, K.-B.; Heo, J.; Nam, J.-M.; Mirkin, C. A. *Angew. Chem., Int. Ed.* **2003**, *42*, 2309.
- (13) Demers, L. M.; Ginger, D. S.; Park, S. J.; Li, Z.; Chung, S. W.; Mirkin, C. A. *Science* **2002**, *296*, 1836.
- (14) Hyun, J.; Ahn, J.; Lee, K. B.; Chilkoti, A.; Zauscher, S. *Nano Lett.* **2002**, *2*, 1203.
- (15) Jung, H.; Kulkarni, R.; Collier, C. P. *J. Am. Chem. Soc.* **2003**, *125*, 12096.
- (16) Liu, X.; Guo, S.; Mirkin, C. A. *Angew. Chem., Int. Ed.* **2003**, *42*, 4785.

Scheme 1



movement can be used to align long macromolecules while patterns are made to improve molecular combing approaches.¹⁷

In a previous study, we reported surface patterning via DPN and HRP-catalyzed aromatic ring coupling reactions of 4-aminothiophenol and tyrosine ethyl ester hydrochloride to form conducting nanowires.¹⁸ In the present study, caffeic acid has been used as a model compound to study surface-induced orientation and subsequent biocatalysis reactions on the nanometer length scale under environmentally friendly reaction conditions. Caffeic acid (3,4-dihydroxycinnamic acid) is found in many fruits, vegetables, seasonings, and herbs, principally in conjugated forms such as chlorogenic acid.¹⁹ Cinnamic acid and its derivatives are used as components in flavors, perfumes, synthetic indigo, and pharmaceuticals. Caffeic acid is a lipoxygenase inhibitor and radical scavenger, which may explain its protective action against cancer cells.²⁰ Caffeic acid and its derivatives, such as chlorogenic acid and caftaric acid, are among the major ortho-diphenolic compounds in plants and act as substrates for polyphenol oxidases or peroxidase.^{21,22}

In addition to the study of the enzymatic polymerization via DPN, regioselective aspects of the surface polymerization of caffeic acid on modified gold surfaces are observed. Scheme 1

illustrates the process. This report demonstrates the important capability of obtaining regioselective control in DPN-patterned nanosystems using surface-mediated reaction control. The resulting structures should lead to new opportunities for improved function in areas of molecular recognition, conductivity, and related applications.

Experimental Section

Materials. Horseradish peroxidase (HRP) (EC 1.11.1.7) (200 units/mg) and hydrogen peroxide (30 wt % water solution) were purchased from Sigma (St. Louis, MO), and a stock solution of 10 mg/mL in 0.1 M phosphate buffer was prepared. Aminothiophenol and 3,4-dihydroxycinnamic acid were purchased from Aldrich (Milwaukee, WI) and used as received. All other chemicals and solvents used were commercially available, of analytical grade or better, and used as received.

Reactions in Solution. HRP-catalyzed polymerization of caffeic acid was carried out at room temperature in 10 mL of MeOH/H₂O (1:1 by volume ratio) mixed solvent, which contained 180 mg of caffeic acid. Two hundred microliters of HRP stock solution was added. A stoichiometric amount of H₂O₂ dilute solution (0.2 M) was added incrementally under vigorous stirring over 1 h. After the addition of hydrogen peroxide, the reaction was left stirring for an additional 2 h, and the precipitates were collected.

Reactions via DPN. Polished silicon chips were coated with 50 nm of titanium followed by ≈300 nm of 99.99% gold (Ted Pella, Redding, CA) by thermal evaporation. The gold substrates were immersed into 1 mM 4-aminothiophenol (*p*-ATP) THF solution for about 30 min. The aromatic primary amine functionalized surfaces were rinsed with acetone several times to remove unbound molecules. A 0.1 M monomer

(17) Nyamjav, D.; Ivanisevic, A. *Adv. Mater.* **2003**, *15*, 1805.

(18) Xu, P.; Kaplan, D. L. *Adv. Mater.* **2004**, *16*, 628.

(19) Olthof, M. R.; Hollman, P. C.; Katan, M. B. *J. Nutr.* **2001**, *131*, 66.

(20) Yagasaki, K.; Miura, Y.; Okauchi, R.; Furuse, T. *Cytotechnology* **2000**, *33*, 229.

(21) Matsumoto, K.; Takahashi, H.; Miyake, Y.; Fukuyama, Y. *Tetrahedron Lett.* **1999**, *40*, 3185.

(22) Cheynier, V.; Basire, N.; Rigaud, J. J. *J. Agric. Food Chem.* **1989**, *37*, 1069.

stock solution was prepared by dissolving caffeic acid in MeOH/H₂O (1:3 v/v) for the DPN “writing ink”. The AFM tip was dipped into the caffeic acid solution for about 20 s and allowed to air-dry. The AFM was used in the “scratching mode” to make patterns, but the piezo voltage was limited such that no actual scratches were made. Parallel lines were drawn on the amine-modified surface at a scratch rate of 0.1 Hz. The caffeic acid was also neutralized by 0.1 M sodium hydroxide at 1:1 molar ratio and patterned on ammonium-functionalized surfaces (Novascan, Ames, IA) in a similar manner as on *p*-ATP surfaces. HRP-catalyzed polymerization was carried out on the DPN-patterned monomers by dipping the substrate into a H₂O₂/enzyme stock solution, which was prepared by mixing 10 mL of 0.01 M H₂O₂ stock solution with 200 μ L of HRP stock solution.

Reactions Based on Microcontact Printing (μ CP). μ CP was used to enlarge the DPN reactions to be able to collect enough polymer product for analysis. Instead of dipping a silicon tip, a PDMS rubber stamp was immersed in a 0.1 M caffeic acid MeOH/H₂O (1:3 v/v) solution and stamped onto an ATP-covered gold substrate to generate surface features. The micron-scale caffeic acid features made by μ CP on *p*-ATP-modified gold surfaces were treated with 10 mL of 0.01 M H₂O₂ containing 200 μ L of HRP stock solution for about 3 min, followed by rinsing with water to remove the enzyme and unreacted H₂O₂. The polymerized features were treated with dilute hydrochloric acid solution to break ionic and hydrogen bonding between caffeic acid and *p*-ATP monolayer. The resulting polymer was eluted from the surface by THF/water (1:1 by volume ratio) mixed solvent for MALDI-TOF analysis.

AFM and EFM Conditions. All imaging and lithography were performed in tapping mode using MPP-13100 probes with a Dimension 3100 SPM equipped with Nanoscope III or IV controllers (Digital Instruments, Santa Barbara, CA). The MPP-13100 probe cantilever length was 125 μ m with a resonant frequency of 525 ± 150 kHz, used to measure high-aspect ratio features. Parallel lines were made at forces varying from 0.35 nN and step point of 0.05 nN to 0.1 nN with a scratch rate of 0.1 Hz. Imaging was achieved at a scan rate of 1.0 Hz. All EFM-phase images were obtained in tapping mode using MESP (magnetic etched silicon probes). The MESP probe cantilever length was 229 μ m with a resonant frequency of 67–83 kHz. The tip was raised 30 nm during EFM scanning with a +5V voltage applied.

Spectroscopic Analyses. Bruker Proflex III MALDI-TOF mass spectrometer (Billerica, MA), equipped with a nitrogen laser of 337 nm and 5 ns pulse width, was used for molecular weight measurements. Dithranol and 2,5-dihydroxybenzoic acid were used as matrixes. X-ray photoelectron spectroscopy (XPS) was carried out with a VG ESCALAB MK II photoelectron spectrometer (VG Scientific, UK) equipped with a concentric hemispherical electron energy analyzer and an Al K α X-ray source ($h\nu = 1486.6$ eV). For XPS analyses, the substrates were not patterned. Instead, macroscopic (1 cm²) gold-coated samples were sequentially immersed in ATP, caffeic acid, and enzyme solutions, as described previously. The base pressure of the instrument was ca. 2×10^{-9} mbar, and photoelectrons were detected normal to the sample plane with a pass energy of 20 eV. To prevent charge buildup on the sample during X-ray irradiation, vacuum-compatible silver paint was used to electrically connect the edges of the sample to the sample stub (which was held at electrical ground). The spectrometer was calibrated using the Au 4f binding energies of clean gold. Because the organic films were thin and the sample surface was electrically grounded, it was not necessary in postanalysis to reference the XPS spectra to a particular peak. FTIR and UV spectra were acquired on a Bruker Equinox 55 FT-IR spectrometer (Billerica, MA) and HP 8452A diode array spectrophotometer (Palo Alto, CA).

Results and Discussion

In our previous studies, 4-aminothiophenol and tyrosine ethyl ester hydrochloride were successfully patterned on gold or modified-gold surfaces. The formation of thiol–Au covalent

bonds or hydrogen bonding provided strong affinity between patterns and substrates. The in situ polymerization of the monomer patterns was achieved by the catalysis of HRP in the presence of hydrogen peroxide. In the present work, caffeic acid was used as a model compound to study surface patterning and enzymatic polymerization via DPN on positively charged surfaces.

The affinity between the ink materials and the substrate plays an important role in surface patterning. The crystalline nature of the caffeic acid, due to hydrogen bonding, prevents it from being adsorbed on substrates. Therefore, it is necessary to find an appropriate solvent to disrupt the hydrogen bonding to permit interactions with substrates used for patterning. A series of solvents, such as DMF, methanol, THF, water, and their combinations, was studied to reduce crystallinity in order to enhance ink–substrate interaction. A methanol–water mixture (1:3 by volume) was used as the optimized solvent.

Caffeic acid nanostructures were formed on primary amine functionalized gold surfaces (Figure 1). The surfaces were primed by immersing the gold-coated silicon chips in 10 mM of 4-aminothiophenol (*p*-ATP) THF solution for about 1 h, followed by complete rinsing with acetone. The primed surface was then functionalized via DPN with caffeic acid. Ionic interactions between the carboxylic acid groups of caffeic acid and primary amine groups of *p*-ATP layers overcome the intermolecular hydrogen bonding of caffeic acid in the crystalline state and facilitate bonding between the caffeic acid and the surface. As described previously, the DPN patterning was performed with nominal 525 kHz tips. Attempts were made to use lower force constant tips, such as Tap300 (300 kHz), but no patterns were observed. To avoid scratching with the higher force constant tip, a low threshold was used, and the step point was increased gradually until reasonable DPN patterns were obtained.

As a catechol derivative, caffeic acid can be oxidized and polymerized by catalysis with HRP in the presence of hydrogen peroxide.⁵ The caffeic acid surface patterns were polymerized in situ by immersion into dilute H₂O₂/HRP solution. Topography and phase images were recorded before and after the polymerization reaction. The parallel lines are 250 nm wide and 58 nm high on average (Figure 1, left). After the enzymatic treatment, the lines are partially overlapped. The apparent line width, defined as the distance between two adjacent troughs in the cross section of the lines, is essentially unchanged after polymerization (Figure 2, left). The line height, however, decreases from 58 to 47 nm. The actual line width increases if deconvolution of the cross section is applied, which is attributed to surface diffusion. This may also explain why the image looks fuzzy after polymerization. The patterned molecules tended to migrate on the surface due to solvation, resulting in decreased line height and line broadening, as we have previously reported.¹⁸

Other surfaces were also investigated as controls, including gold and ammonium or MHA (16-mercaptohexadecanoic acid) modified gold. Poor surface patterns were obtained on MHA-coated surfaces due to weak hydrogen-bonding interactions. Ammonium-modified surfaces were better than the carboxylic acid functionalized surfaces, but the caffeic acid tended to aggregate, resulting in the formation of discontinuous lines. Sodium hydroxide neutralized caffeic acid was also used to draw

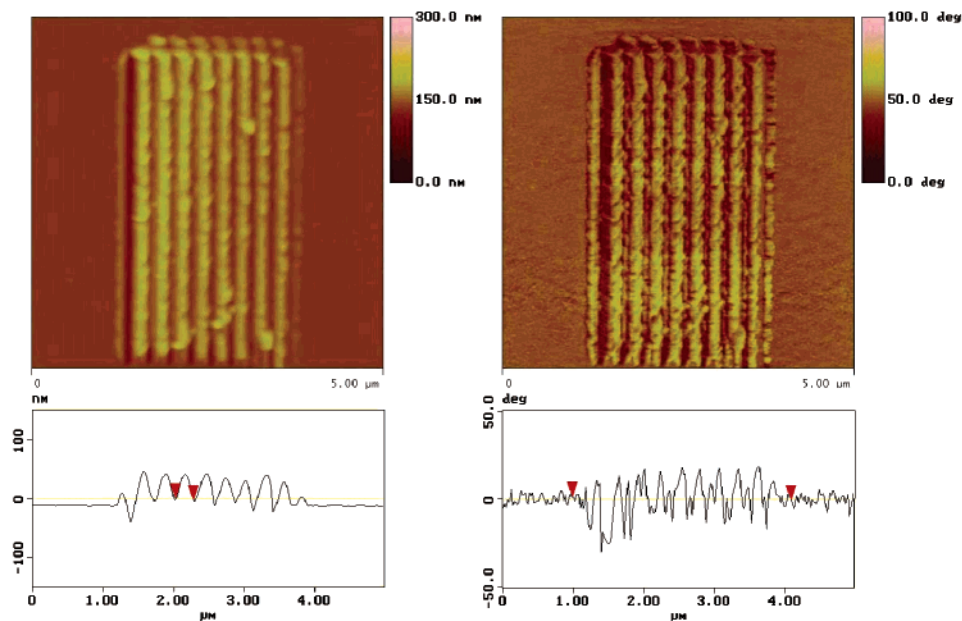


Figure 1. AFM images of caffeic acid monomer patterned on *p*-ATP-modified gold surfaces: (left) topography image and (right) phase-lag image.

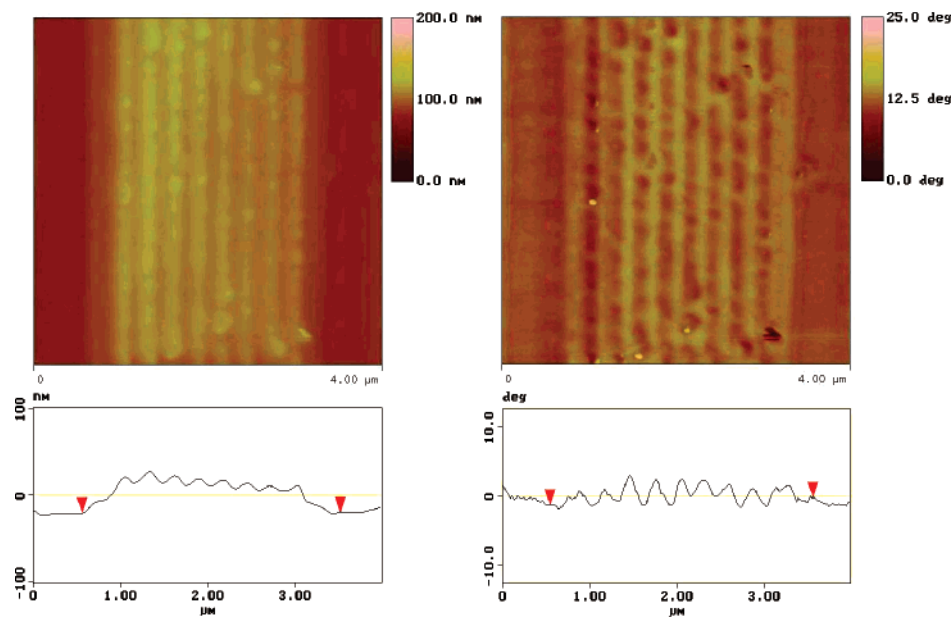


Figure 2. AFM images of caffeic acid patterns on *p*-ATP-modified gold surfaces after HRP-catalyzed polymerization: (left) topography image and (right) phase-lag image.

lines on ammonium surfaces, and the patterns are shown in Figure 3. These results are similar to those of Figure 1, but there are some discontinuities along the lines. In the case of neutralized caffeic acid on ammonium surfaces, trenches were formed, apparently due to the relatively poor adhesion between the neutralized caffeic acid and ammonium layers. These results demonstrate that the *p*-ATP and caffeic acid system has optimum interfacial affinity.

AFM phase lag images were acquired simultaneously with the topography images. Phase signals are more sensitive than the amplitude signals that were used to plot the height images and record the sinusoidal lag caused by the changes in the physical properties of the surfaces, such as the hardness and viscosity. The polymerized caffeic acid would be expected to be more rigid than the monomer, since the diphenolic moiety is coupled to form a rodlike macromolecule. The phase lag value

decreases from 30.6° to 4.4° after the HRP/H₂O₂ treatment, consistent with polymerization of the caffeic acid (Figures 1 and 2, right). The *p*-ATP self-assembled monolayer without caffeic acid patterns was exposed to HRP/H₂O₂ as a control (Figure 4). There is no significant change in phase lag after treatment. This indicates that the decrease of phase lag of the patterns is not caused by interference of *p*-ATP monolayer but is due to polymerization of caffeic acid.

To confirm the formation of caffeic acid polymer, electrostatic force microscopy (EFM) phase images were acquired before and after the oxidative coupling of the surface-patterned caffeic acid (Figure 5). The average phase lag decreased from $5.8^\circ \pm 0.7^\circ$ to $4.1^\circ \pm 0.5^\circ$ due to the ring coupling. The more extended conjugated structure of the polymer is expected to result in a more conductive surface. Since the gold substrate is conductive, more charge removed from the pattern is expected to decrease

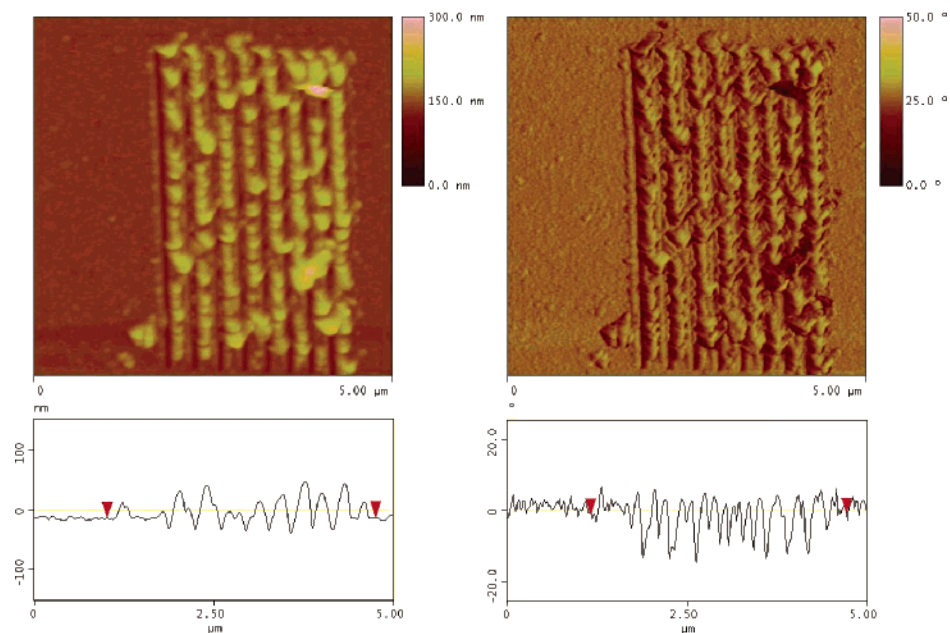


Figure 3. AFM images of sodium hydroxide-neutralized caffeic acid patterns on ammonium-functionalized surfaces: (left) topography and (right) phase-lag image.

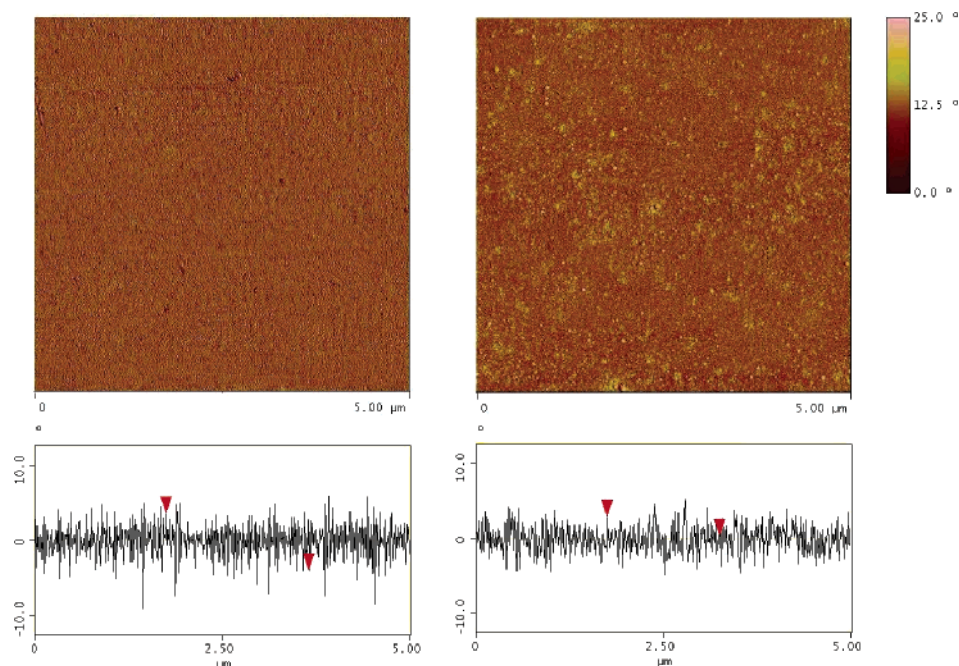


Figure 4. AFM phase-lag images of *p*-ATP self-assembled monolayer: (left) before and (right) after HRP/H₂O₂ treatment as control.

the sample–tip capacitance. The reduced electrostatic force leads to a decreased phase lag of the sinusoidal signals applied to the AFM tip.²³ These results support the conclusion of successful polymerization of caffeic acid after the HRP/H₂O₂ treatment. As a control, the EFM images of the *p*-ATP monolayer before and after HRP/H₂O₂ treatment have also been recorded (Figure 6). The very small phase lag values and the identical profiles of the cross section of selected areas indicate that the decrease of the phase lag signal is only caused by the polymerization of caffeic acid.

Since only a very small amount of product is formed during enzymatic polymerization of nanoscale patterns generated by DPN, microcontact printing can be used to simulate the reaction at a larger scale in order to collect enough polymers for characterization and structural analysis. During the DPN process, the function of the AFM tip is not limited to transport of ink. The surface patterned molecules may be aligned when the tip travels over the surface and writes the patterns. This can help rearrange the ink molecules into a more organized structure along the DPN patterns when they bond to the surface. μ CP would have this benefit since the driving force is induced by the SAM surface. To understand the in situ polymerization

(23) Lei, C. H.; Das, A.; Elliott, M.; Macdonald, J. E. *Appl. Phys. Lett.* **2003**, *83*, 482.

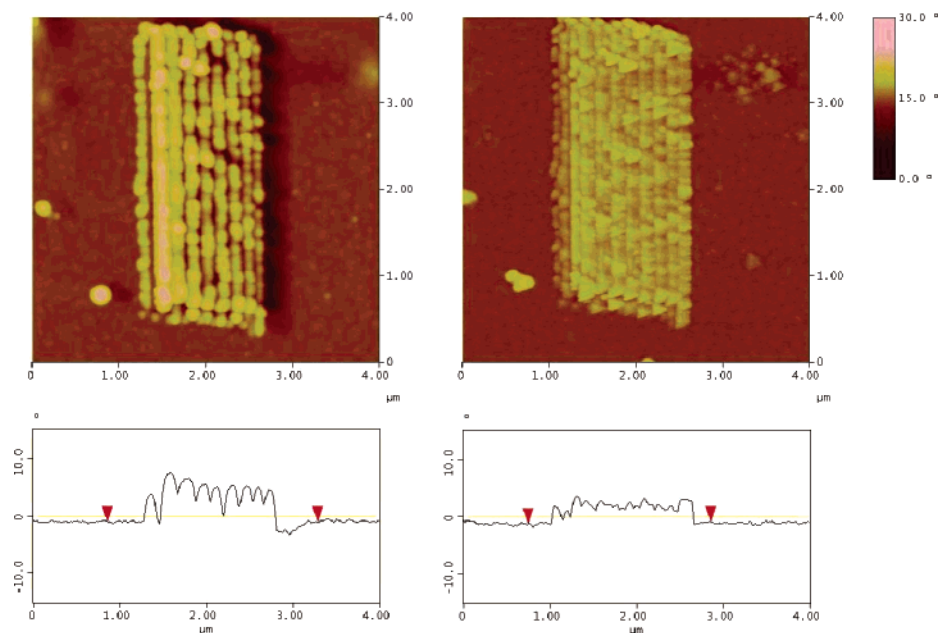


Figure 5. EFM phase images of caffeic acid patterned on *p*-ATP-modified gold surfaces: (left) before and (right) after HRP/H₂O₂ treatment.

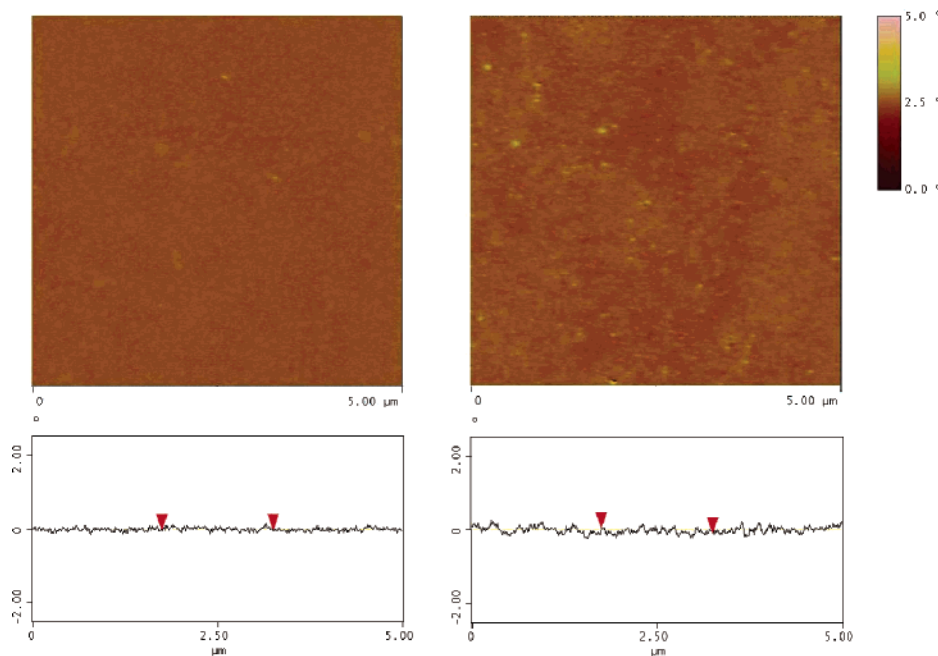


Figure 6. EFM phase images of *p*-ATP self-assembled monolayer: (left) before and (right) after HRP/H₂O₂ treatment as control.

behavior and the effects of surface orientation, further characterization was performed.

Dithranol was used as a matrix for MALDI-TOF analysis of the polymer. The polymerized caffeic acid from microcontact printed patterns contained molecular masses up to at least 1100 Da (Figure 7). In the MALDI spectrum, the large peak at around 230 Da is the matrix peak. The difference between each group of peaks is the molecular mass of the monomer, caffeic acid. Small peaks adjacent to the major peak of each mer are the fragment peaks caused by the loss of end groups, such as hydroxy or carboxylic acid groups. The microcontact printed features typically have a thickness of 250–500 nm. It is unlikely that HRP/H₂O₂ can penetrate this deeply. But when the patterns are exposed to HRP/H₂O₂, some loosely bound or (initially) unpolymerized molecules may diffuse into solution, resulting

in decreased thickness and allowing HRP to penetrate. It may be expected that low molecular weight species would form deeper in the caffeic acid layer, since less HRP/H₂O₂ is expected to penetrate those regions. The MALDI spectrum shows that the polymeric product contains dimer, trimer, larger oligomers, and higher molecular weight species. The trimer is dominant, consistent with HRP-catalyzed free radical induced polymerization of phenolic compounds.²⁴

Analysis of the chemistry of the in-situ polymerized surfaces was performed with XPS. Because of the technique's spatial resolution limitations, the experiments were performed on macroscopic (1 cm² × 1 cm²) gold-coated silicon wafer samples. While the main subject of this paper is the patterning of

(24) Xu, P.; Kumar, J.; Samuelson, L.; Cholli, A. L. *Biomacromolecules* **2002**, *3*, 889.

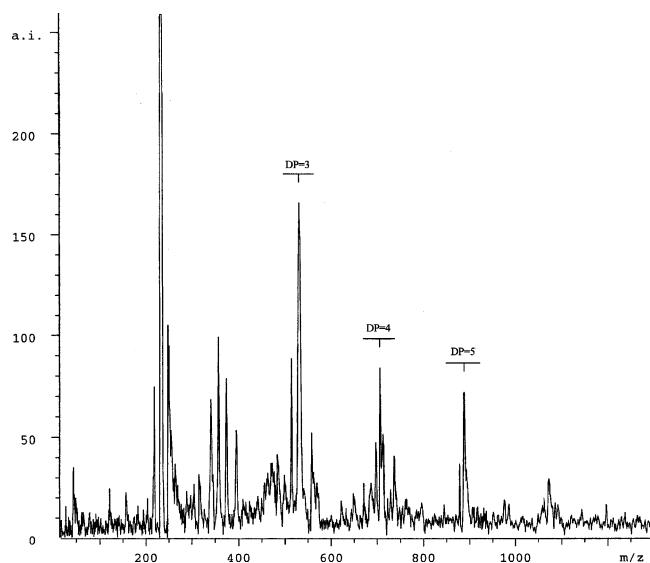


Figure 7. MALDI-TOF mass spectrum of poly(caffeic acid).

polymeric caffeic acid on *p*-ATP, the latter is also a substrate for HRP, and the possibility of the *p*-ATP monolayer being involved in the reaction must also be considered.

It was demonstrated previously that HRP/ H_2O_2 -induced polymerization of monolayer ATP occurs.¹⁸ Figure 8 shows C 1s and N 1s XPS spectra of a monolayer of *p*-ATP self-assembled on a gold surface. The C 1s binding energy at 284.20 eV (fwhm = 2.06 eV) is associated with the hydrocarbons within the *p*-ATP monolayer. Immersion of the ATP-covered gold sample in 10 mL of 0.01 M aqueous H_2O_2 solution mixed with 200 μL of HRP stock solution for 3 min, followed by rinsing with water, resulted in dramatic changes in both the carbon and nitrogen XPS peaks (top spectra in Figure 8). Deconvolution of this C 1s peak (fwhm = 2.70 eV) shows three components at 284.45, 285.80, and 287.78 eV, with fwhm of 2.45, 1.18, and 2.39 eV, respectively. The middle spectra correspond to a control experiment in which an ATP-covered gold sample was immersed in 10 mL of water containing 200 μL of HRP stock solution (without H_2O_2). In the case of the C 1s peak (fwhm = 2.50 eV), deconvolution also shows three components at 284.42, 285.88, and 287.42 eV, with fwhm of 1.93, 1.83, and 3.60 eV, respectively. Because hydrogen

peroxide is required to induce polymerization,² no polymer is present in the control sample. The similarity of the control and polymer samples suggests that nonspecifically bound HRP is present on the surface of both the control and polymer sample. This conclusion is substantiated by the corresponding N 1s data. For *p*-ATP assembled on gold, the N 1s spectrum has maximum intensity at 399.06 eV (fwhm = 1.50 eV). The HRP-only control and polymer spectra are similar to each other and peaked at ca. 400.10 eV with fwhm of 1.90 eV. The lower signal-to-noise ratio in the case of the ATP-covered gold surface (bottom spectrum) is due to having only a single monolayer of molecules. The control and polymer samples exhibit higher N 1s signals due to the thicker nitrogen-containing organic layers resulting from adsorbed HRP protein.

Figure 9 displays corresponding XPS data for a monolayer of *p*-ATP self-assembled on gold which was immersed for 3 min in a 0.1 M caffeic acid monomer MeOH/ H_2O (1:3 v/v) solution and then rinsed. The bottom spectra refer to the samples prior to polymerization, and the middle and upper ones correspond to the HRP (without H_2O_2) control and the HRP/ H_2O_2 polymerized surfaces, respectively. The O 1s XPS spectra are also included. In the case of the C 1s data, the spectra broadened after exposure to HRP and polymerization. Caffeic acid adsorbed on ATP exhibits a C 1s peak at 284.00 eV (fwhm = 2.35 eV). For the control sample, the spectrum (overall fwhm = 2.90 eV) is similar to what was observed in the case of the ATP without caffeic acid. Deconvolution shows peaks at 284.58, 286.04, and 287.77 eV with fwhm of 2.07, 1.72, and 3.11 eV, respectively. In the case of the polymer, the spectrum is broader (overall fwhm = 3.20 eV), and deconvolution shows only two peaks at 285.34 and 287.15 eV, with fwhm of 2.34 and 4.20 eV, respectively.

In the case of the nitrogen spectra, very weak N 1s intensity is observed for the caffeic acid/ATP sample. This is due to the nitrogen of the ATP being covered by a thick enough layer of caffeic acid such that the photoelectrons in the ATP layers are almost completely attenuated. HRP immersion leads to an enhancement in the N 1s signal (peak at 400.20 eV with fwhm = 1.80 eV) due to HRP adsorption on top of the caffeic acid layer. The polymerized spectrum shows a slight shift and broadening (peak at 400.50 eV, fwhm = 2.00 eV). In the case of the oxygen XPS data, the ATP/caffeic acid surface and this

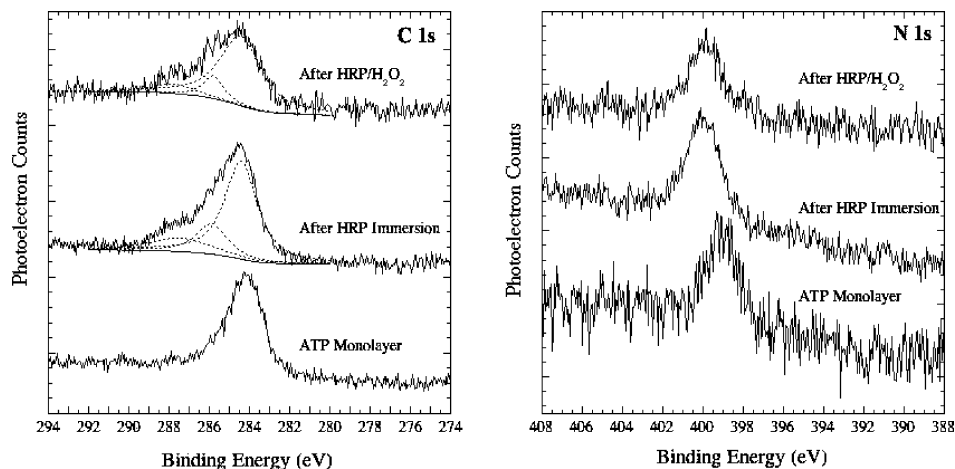


Figure 8. Al $K\alpha$ XPS spectra of the C 1s and N 1s regions of *p*-ATP self-assembled on gold, a similar sample immersed in an aqueous HRP solution (without H_2O_2), and the polymerized ATP sample formed by immersion in HRP/ H_2O_2 . The dashed lines show the deconvolutions of the C 1s peaks. The binding energy is referenced to the spectroscopic Fermi level.

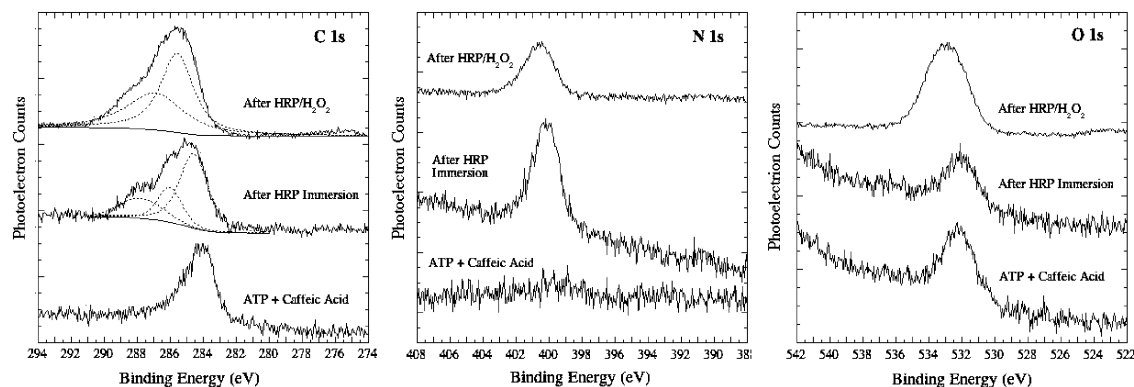


Figure 9. Al K α XPS spectra of the C 1s, N 1s, and O 1s regions of a caffeic acid monomer-covered ATP/Au sample, a similar sample immersed in an aqueous HRP solution (without H₂O₂), and the polymerized sample formed by immersion in HRP/H₂O₂. The dashed lines show the deconvolutions of the C 1s peaks. The binding energy is referenced to the spectroscopic Fermi level.

surface following immersion in HRP solution are similar, with peak binding energy at ca. 532.1 eV (fwhm = 2.40 eV). This peak broadens (fwhm = 2.90 eV) and shifts to 532.8 eV following polymerization. The shift and broadening of the O 1s spectrum possibly may be associated with polymerization and trapped hydrogen peroxide within the film. Peak integration, weighted by appropriate sensitivity factors, indicates O/C atomic ratios of 0.29 and 0.41 for the caffeic acid monomer and polymer films, respectively.

The XPS studies indicate that HRP is adsorbed on both ATP and ATP/caffeic acid surfaces. The C 1s spectrum of the polymerized sample shows a broadening of the high binding energy component at 287.15 eV and is likely due to the coupling of adjacent benzene rings or oxygen incorporation (from hydrogen peroxide) and the formation of C–O or C=O bonds.^{25,26}

UV–vis absorbance of poly(caffeic acid) obtained by in situ surface polymerization, the subject of this paper, and solution polymerization is compared in Figure 10. Also included is a monomer spectrum; in this case, the monomer was patterned on *p*-ATP monolayer by μ CP without any treatment. In the monomer spectrum (1), the absorbance peak at 286 nm is attributed to the π conjugation of the double bond and benzene ring in caffeic acid. The monomer patterns were treated with H₂O₂ without the presence of HRP as a control (spectrum 2). The spectrum retains a similar profile and no peak shift is observed. After the caffeic acid is polymerized in solution (spectrum 4), the peak at 286 nm broadens and red shifts to 296 nm, indicating the increment of the conjugation length which was induced by the oxidative coupling polymerization. A new peak appears at 326 nm and can be associated with the n – π^* transition due to the C–O–C coupling.^{27,28} The absorbance spectrum of caffeic acid monomer at 286 nm exhibits a red-shift to 292 nm following in situ surface polymerization, which is attributed to the increased conjugated structure caused by the ring coupling reaction. With the increased conjugation length and formation of polymers, less energy is required for the π – π^* and n – π^* transition or electron delocalization, which results

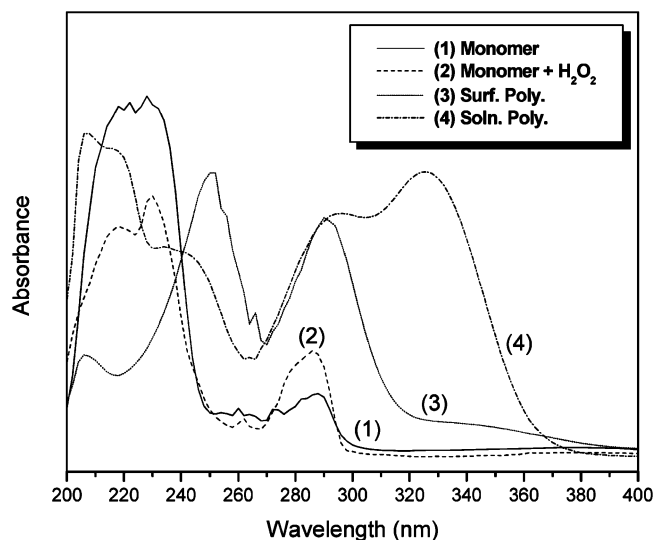


Figure 10. UV–vis absorbance of the caffeic acid and its polymeric products: (1) solid line, monomer; (2) dashed line, monomer exposed to H₂O₂ without the presence of HRP; (3) dotted line, in situ surface polymerization; and (4) dashed–dotted line, polymerized in solution.

in the red-shift. The peak is much broader than that of the monomer and its control at 286 nm, indicating the presence of many polymeric species with different molecular weights, consistent with the MALDI-TOF mass spectrometry results. Note that spectrum 3 is not as broad as observed for solution polymerization. This indicates a lower degree of polymerization of the product obtained in the surface reactions compared to solution polymerization. In spectrum 3, new peaks at 252 nm and a plateau from 326 nm to \sim 384 nm are observed. These new peaks are attributed to the formation of an *o*-quinone structure, which is consistent with the results of the oxidation of caffeic acid.²⁹ But in spectrum 4, no quinone absorption was found. The plateau at about 244 nm was attributed to the red-shift from 230 nm (monomer spectrum) due to the extended conjugation.

The FT-IR spectra of caffeic acid and the products of the μ CP surface and solution polymerization samples are shown in Figure 11. The caffeic acid monomer patterns were also treated with H₂O₂ without the presence of HRP as a control. The spectrum of the control sample exhibits similar profiles as the monomer. The absorption peaks between 1450 and 1620 cm^{–1}

(25) Goldberg, M. J.; Clabes, J. G.; Kovac, C. A. *J. Vac. Sci. Technol. A* **1988**, *6*, 991.

(26) Briggs, D. *Surface Analysis of Polymers by XPS and static SIMS*, Cambridge University Press: Cambridge, 1998.

(27) Hulubei, C.; Cozan, V.; Bruma, M. *High Performance Polym.* **2004**, *16*, 405.

(28) Radziszewski, J. G.; Gil, M.; Gorski, A.; Spanget-Larsen, J.; Waluk, J.; Mroz, B. *J. Chem. Phys.* **2001**, *115*, 9733.

(29) Cheynier, V.; M., M. *J. Agric. Food Chem.* **1992**, *40*, 2038.

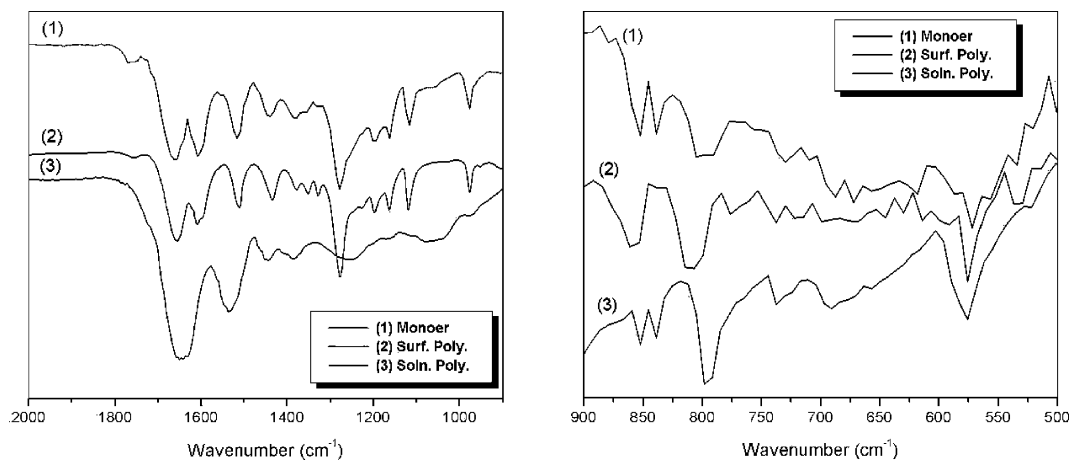


Figure 11. FT-IR spectra of caffeic acid and its polymeric products: (1) monomer, (2) in situ surface polymerization, and (3) solution polymerization.

are associated with the aromatic ring C=C stretching vibration bands. The vibration bands of the carboxylic group appeared at 1660 cm^{-1} . The absorption peak at 1280 cm^{-1} is attributed to the C–O stretching vibration bands. The absorption peaks at 1200 and 1160 cm^{-1} are the phenolic O–H deformation and stretching vibration bands, respectively. Particularly, in the spectrum of solution polymerized caffeic acid (spectrum 3), the C–O–C stretching vibration peak of the phenyl ester is observed at 1255 and 1065 cm^{-1} ,^{5,30} which is not found in spectrum 2. However, the existence of phenolic structures is observed in spectrum 2. These results support the above conclusion that hydroxy groups within the benzene ring are not involved in the surface polymerization reaction. In the benzene ring fingerprint region ($900\text{--}650\text{ cm}^{-1}$), the peaks at 860 and 810 cm^{-1} associated with the out-of-plane deformation vibrations band (1 isolated H atom) are observed in spectrum 2, which indicates that the formation of pentasubstitution in the benzene ring is due to C–C ring coupling. Spectrum 3 has a similar profile as spectrum 1. The absorptions at 850 , 840 , and 800 cm^{-1} are attributed to the out-of-plane deformation vibrations of two isolated H atoms. This suggests that the formation of the polymeric product is mainly through C–C ring coupling in the surface reaction, while a majority of C–O–C aromatic ethers is observed in the solution polymer spectrum.

The C–O–C coupling, which is well-known from enzymatic polymerization of phenolic monomers in solution, was not observed in the surface reactions. The proposed structures of the polymeric products are shown in Figure 12. Surface organization plays an important role in templating monomers and restricting some reaction positions. On the *p*-ATP monolayer, caffeic acid was bonded by ionic interactions with the diphenolic moiety away from the surface. According to free radical resonance, the formation of the quinone features facilitates C–C ring coupling. The structural difference of the polymeric product was dictated by the stereoregularity and the reaction environment.

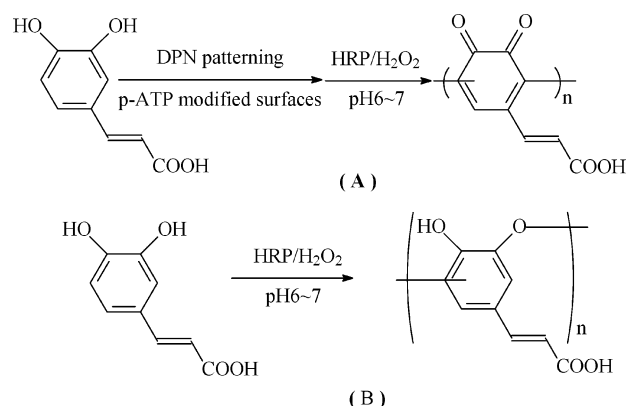


Figure 12. The proposed structures of the final polymeric products (A) obtained by surface polymerization and (B) obtained by solution polymerization.

Conclusions

Nanoscale surface patterning of caffeic acid was successfully achieved on *p*-ATP modified gold surfaces by DPN. HRP-catalyzed polymerization was applied on the patterned caffeic acid features, and EFM data indicated increased conjugation length as a result of enzymatic reaction. The polymeric products were determined by MALDI-TOF mass spectroscopy, and molecular masses up to 1200 Da were found. XPS surface analysis indicated that nonspecifically bound HRP is also present in the surface-polymerized sample. Comparison of the polymeric products obtained from surface and solution polymerization was performed with UV–vis and FT-IR. UV absorbance and FT-IR spectra indicated that the hydroxyls within the caffeic acid benzene ring, which form quinone structures during in situ surface polymerization, were not involved in building the polymer backbone. C–O–C coupling was observed in the solution-polymerized products. This structural difference was attributed to the surface organization and orientation provided by the DPN process.

Acknowledgment. Support from the Air Force MURI program (F49620) is gratefully acknowledged.

JA051637R

(30) Dubey, S.; Singh, D.; Misra, R. A. *Enzyme Microb. Technol.* **1998**, *23*, 432.